International Journal of Modern Physics E
Vol. 20, No. 11 (2011) 2361–2375

DOI: 10.1142/S021830131102037X

World Scientific
www.worldscientific.com

MEASUREMENT OF PHOTOFISSION CROSS-SECTION OF ^{238}U USING MICROTRON FACILITY

H. G. RAJ PRAKASH*,†,¶, GANESH SANJEEV†, K. B. VIJAY KUMAR†,
H. G. HARISH KUMAR‡, K. SIDDAPPA†, B. K. NAYAK§ and A. SAXENA§

*Department of Engineering Physics,
JNN College of Engineering, Shimoga-577 204, India
†Microtron Center, Department of Physics, Mangalore University,
Mangalagangotri-574 199, India
‡Department of Engineering Physics, SJM Institute of Technology,
Chitradurga-577 502, India
§Nuclear Physics Department, Bhabha Atomic Research Center,
Mumbai 400 056, India
¶prakashraj06@rediffmail.com

Accepted 13 September 2011

Photofission cross-section of ^{238}U was measured using bremsstrahlung radiation energy 7.4–9.0 MeV with energy step of 0.4 MeV by employing Lexan polycarbonate film as solid state nuclear track detector (SSNTD). The photon intensity from the Microtron accelerator at a distance of 15 cm from the bremsstrahlung converter (tantalum target) facility was estimated to be 10^{10} photons/sec using the code EGS-4. In this paper, details of the fission fragment angular distribution measurements of ^{238}U target using Lexan polycarbonate have been discussed. The photofission cross-section was calculated using the angular distribution of fission fragments and the results were compared with those obtained using the code EMPIRE-II and various barrier parameters of the RIPL-1, RIPL-2 libraries and with the new analytical fission barrier formula based on the Hugenholtz–Van Hove theorem. The present experimental measurements were in good agreement with the results obtained from the Empire-II code predictions for potential parameter taken from RIPL-1 and a newly developed analytical fission barrier formula.

Keywords: Fission bremsstrahlung; ^{238}U(γ, f); angular distributions; fission yields; SSNTD; photofission cross-sections; photon difference method.

PACS Number(s): 25.85.Jg

1. Introduction

Photofission is interesting by means of studying the fission process, since it possesses some unique properties, such as simplicity of the spectrum of angular momentum transfer to the nucleus undergoing fission. Near fission threshold, most excitation energy is converted into nuclear deformation energy and so fission proceeds through only a few low-lying fission channels. This makes interpretation of experimentally measured cross-sections easier for photon induced fission than fission induced by

other particles, such as neutrons.[1] There are many reports on photofission of ^{238}U carried out using bremsstrahlung, quasimonochromatic photons from positron annihilation, variable energy Compton scattered gammas, proton capture gammas and tagged photons.[2] In most of these experiments, only photofission cross-sections have been measured. From the review of the Rabotnov *et al.*,[3] fission fragment angular distribution studies of the heavier actinides indicate a negligible amount of quadrupole component in the energy region 6–9 MeV, while other measurements[5,6] do indicate the presence of a significant electric quadrupole component. It is our interest to study the dipole and quadrupole contribution in photofission near threshold to understand the transition state properties of the fissioning nuclei. With this aim, we measured the angular distribution of fission fragments of ^{238}U using bremsstrahlung radiation over the energy range 7.4–9.0 MeV. The present measurements were compared with the results of theoretical EMPIRE-II nuclear reaction code[6] prediction for various potential parameters, a newly developed analytical fission barrier formula[7] and results taken from the EXFOR library.[8] Microtron accelerator at the Mangalore University provides variable energy bremsstrahlung radiation to carry out photofission experiment near threshold.

2. Methodology

The fission fragment angular distribution of ^{238}U nuclei measurements were performed using bremsstrahlung radiation from the Microtron installed at the Mangalore University. The extracted electron beam hit a water-cooled bremsstrahlung converter, made of 0.188 cm-thick tantalum target. The electron beam is supplied by a pulsed electron gun at a pulse repetition rate of 50 Hz. The maximum current of the analyzed beam is 4 μA and electron energy resolution is $\pm$28 keV. The detail of the machine has been published elsewhere.[9–11] The electron beam was monitored by a FCT (fast current transformer), placed before the bremsstrahlung converter for photofission experiments. Bremsstrahlung yield simulation was carried out using Monte Carlo EGS-4 code.[12] The method followed for target thickness estimation, angular distribution, and bremsstrahlung yield of various energy estimation was discussed elsewhere.[13]

A ^{238}U target was placed in the centre of a cylindrical vacuum chamber, making an angle of 45° with the incident beam direction. The target was made by depositing 200 μg/cm^2-thick ^{238}U on an aluminum backing. Amount of electrodeposited ^{238}U target on aluminum was determined by X-ray diffraction method. A simple illustration of the target geometry is shown in Fig. 1. The fission chamber used in the experiment was 8 cm high and had a diameter of 8 cm. The fission fragments were detected using Lexan polycarbonate films placed at different angles with respect to the incident beam direction and the target was irradiated for 5 h. After irradiation the Lexan films were cut into equal strips and etched in 6 N NaOH solution for about 1 h to develop the fission tracks.[14] These etched Lexan films were washed, dried and analyzed under optical microscope with a magnification of

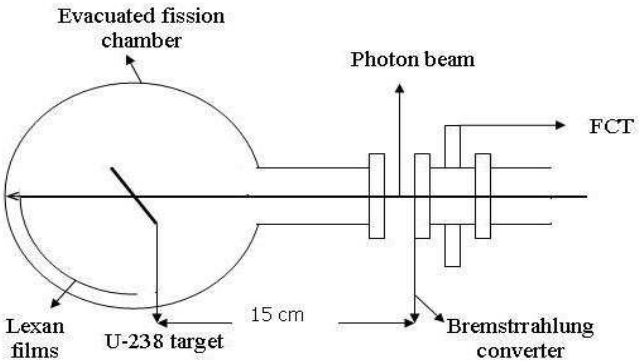

Fig. 1. Schematic diagram of experimental setup.

400× for the tracks formed during irradiation. During photofission experiments the possible contamination of the bremsstrahlung beam with secondary electron and neutrons were estimated using EGS-4 code and it was found to be negligible.[15]

3. Results and Discussion

The measurements of fission fragment angular distribution of ^{238}U nuclei as a function of the maximum bremsstrahlung end point energy ($E_{\max}$) is as shown in Fig. 2. The fission fragment angular distributions were obtained at various energies by normalizing the fission track counts to the solid angle and photon intensity. The photon

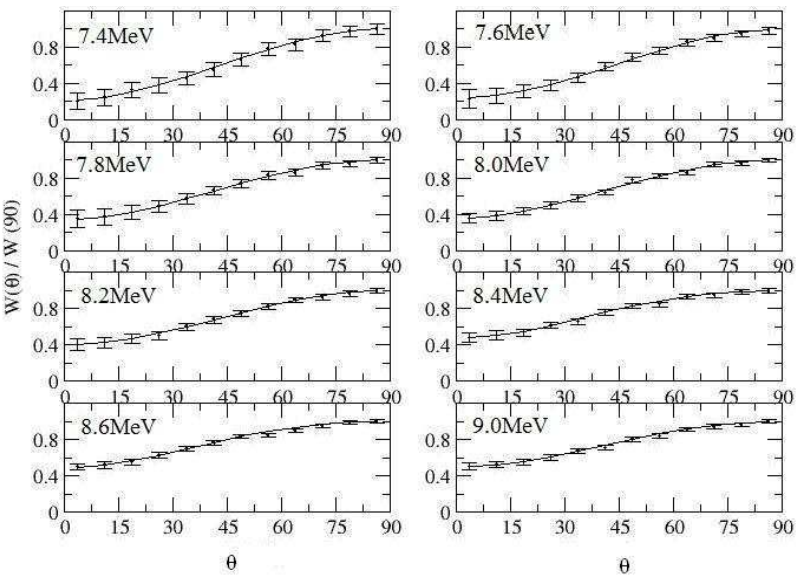

Fig. 2. Fission fragment angular distribution of ^{238}U induced by bremsstrahlung in the energy range 7.4–9.0 MeV.

intensity was estimated to 10^{10} photons/sec along the beam axis at all energies using EGS-4 code.[12] The measured fission fragment angular distributions were least square fitted with the expression[16]:

$$W(\theta) = a + b\sin^2\theta + c\sin^2 2\theta\,. \tag{1}$$

The solid curves are the curves determined by least square fit to the data using Eq. (1). The individual coefficient of Eq. (1) was determined by the least square fit and is listed in Table 1. The experimental error shown in Fig. 2 has been determined by using statistical error in detector output which is given by $1/\sqrt{N}$, where "N" is the number of counts. The statistical error is low at high energies and increases due to smaller numbers of events collected at low energies. The standard error propagation formula is,

$$\sigma_u = \sqrt{\left(\frac{\partial u}{\partial x}\right)^2 \sigma_x^2 + \left(\frac{\partial u}{\partial y}\right)^2 \sigma_y^2 + \cdots}\,. \tag{2}$$

The values of fitted coefficients a and b in Table 1 agree within experimental error with the values obtained by Rabotnov *et al.*[3] who had employed the technique quite similar to the one described here with the exception that the fragment emission direction was determined by track angles making use of SSNTD technique. The values of "c" obtained by Rabotnov *et al.*[3] also agreed within the experimental error to our present measurements. The present experimental results are also shown in Table 2. Figure 3 shows the ratio b/a which represents contribution of the dipole in photo absorption and its variation as a function of end point energy ($E_{\max}$) of bremsstrahlung photons and hence are compared with the values of Rabotnov *et al.*[17] and Baerg *et al.*[18]

Figure 3 clearly shows that the anisotropy decreases with increasing energy. According to Bohr hypothesis (Aage Bohr, 1956),[19] the ratios b/a decreases with increasing excitation energy. This result agrees with our experimental measurements. The anisotropy values (b/a) are in good agreement with the measurements of Rabotnov *et al.*,[17] and the obtained values are quite high in comparison with the Baerg *et al.*[18]

Table 1. Values of the coefficients a, b and c obtained by fitting the experimental data to the function $W(\theta) = a + b\sin^2\theta + c\sin^2 2\theta$.

Energy (MeV)	a	b	c
7.4	0.217 ± 0.056	0.783 ± 0.34	0.0212 ± 0.002
7.6	0.240 ± 0.041	0.760 ± 0.33	0.0002 ± 0.003
7.8	0.342 ± 0.055	0.658 ± 0.32	0.0311 ± 0.002
8.0	0.357 ± 0.039	0.643 ± 0.23	0.0259 ± 0.003
8.2	0.400 ± 0.064	0.600 ± 0.3	0.0196 ± 0.002
8.4	0.478 ± 0.068	0.522 ± 0.25	0.0570 ± 0.002
8.6	0.490 ± 0.049	0.510 ± 0.18	0.0570 ± 0.003
9.0	0.500 ± 0.061	0.500 ± 0.18	0.0225 ± 0.001

Table 2. Values of the coefficients a, b and c obtained by fitting the experimental data to the function $W(\theta) = a + b\sin^2\theta + c\sin^2 2\theta$.

Energy (MeV)	a	b	c
7.38	0.708 ± 0.013[a]	0.3292 ± 0.042	0.057 ± 0.008
	0.66 ± 0.08[b]	0.38 ± 0.07	0.64 ± 0.25
	0.31 ± 0.04[c]	0.786 ± 0.008	0.044 ± 0.008
	0.217 ± 0.056[d]	0.783 ± 0.34	0.0212 ± 0.002
7.64	0.689 ± 0.008	0.424 ± 0.024	0.051 ± 0.004
	0.67 ± 0.11	0.40 ± 0.10	0.47 ± 0.36
	0.359 ± 0.004	0.750 ± 0.007	0.041 ± 0.008
	0.240 ± 0.041	0.760 ± 0.33	0.0002 ± 0.003
7.91	0.832 ± 0.018	0.217 ± 0.054	0.04 ± 0.01
	0.63 ± 0.24	0.48 ± 0.20	0.39 ± 0.43
	0.382 ± 0.006	0.641 ± 0.007	0.033 ± 0.007
	0.357 ± 0.039	0.643 ± 0.23	0.0259 ± 0.003
8.99	0.839 ± 0.007	0.215 ± 0.021	0.033 ± 0.004
	0.88 ± 0.08	0.13 ± 0.07	0.24 ± 0.24
	0.554 ± 0.007	0.495 ± 0.008	0.017 ± 0.008
	0.500 ± 0.061	0.500 ± 0.18	0.0225 ± 0.001

[a]The constants appearing in the first row for each energy are from Ref. 36.
[b]The constants appearing in the second row for each energy are from Ref. 19.
[c]The constants appearing in the third row for each energy are interpolated from the data in Ref. 17.
[d]Measurements of present investigation.

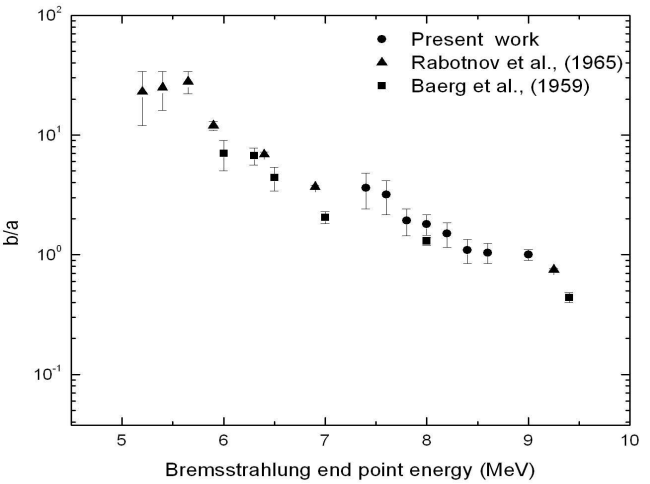

Fig. 3. Energy dependence of b/a for the photofission of ^{238}U.

Figure 4 shows the variation of c/b as a function of bremsstrahlung end point energy range. The quadrupole absorption gives a small, but systematically different from zero contribution at all energies. The statistical error is large so as to reach

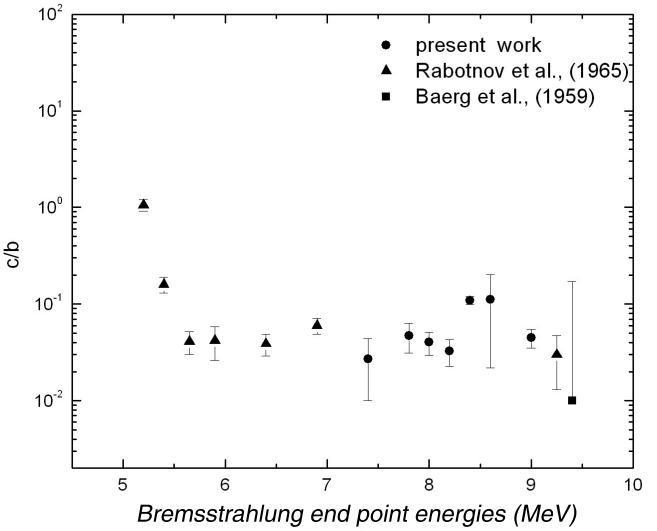

Fig. 4. Energy dependence of c/b for the photofission of ^{238}U.

any conclusion about its behavior as a function of energy. It can be said that "c" seems to be almost constant in the energy range 7.4–9.0 MeV.

3.1. *Anisotropy calculations*

Figure 5 is a plot of comparison of theoretical and experimental values of b/a for photofission of ^{238}U irradiated by bremsstrahlung radiation. The anisotropy is calculated using the equation

$$\frac{b}{a}+\frac{1}{2}=\frac{\displaystyle\int_0^{E_{\max}}\left\{\begin{array}{c}E^3(E_{\max}-E)^2T_{\lambda f}(1,-,0,E)\\ T_{\lambda\gamma}(1,-,E)+T_{\lambda f}(1,-,0,E)+2T_{\lambda f}(1,-,1,E)\end{array}\right\}}{\displaystyle\int_0^{E_{\max}}\left\{\begin{array}{c}2E^3(E_{\max}-E)^2T_{\lambda f}(1,-,0,E)\\ T_{\lambda\gamma}(1,-,E)+T_{\lambda f}(1,-,0,E)+2T_{\lambda f}(1,-,1,E)\end{array}\right\}}. \tag{3}$$

The anisotropy values substantially deviated at the higher energies. The discrepancies arise due to theoretical values of b/a are forced toward the asymptotic value of $1/2$ at higher energies, since barrier penetrabilities approach unity. However, the experimental value of b/a is greater than one at higher photon energies. We assume that this is due to the opening of additional dipole $K \neq 0$ fission levels. This is indicated by a decrease in b/a as is evident by the experimental data.

To make a quantitative analysis of the measured fission fragment angular distributions, it is assumed that $J = 1^-$, $K = 0$ and $J = 1-$, $K = 1$ are responsible for the angular distributions and $J = 2^+$ and $K = 0$ states lead to a quadrupole absorption which gives a small but systematically different from zero contribution at all energies. From values of the coefficients obtained from the least square fit, we

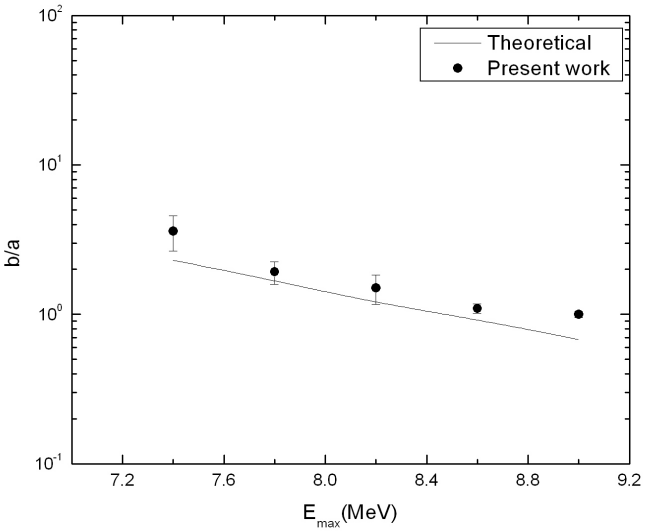

Fig. 5. Comparison of theoretical and experimental values of b/a for photo fission of ^{238}U with bremsstrahlung. The theoretical values are derived from Eq. (3) [• — Present experimental results].

can determine the three angular components $Y_a(E_{\max})$, $Y_b(E_{\max})$ and $Y_c(E_{\max})$ of the yield, which corresponds to isotropic, dipole and quadrupole terms which are related by Eq. (5) and are shown in Fig. 6. These are related by the equations,

$$\begin{aligned} Y &= Y_a + Y_b + Y_c\,, \\ Y_a &= \frac{Y_a}{v}\,, \\ Y_b &= Y\left(\frac{2b}{3v}\right)\,, \\ Y_c &= Y\left(\frac{8c}{15v}\right)\,, \\ v &= \left(a + \frac{2}{3}b + \frac{8}{15}c\right)\,. \end{aligned} \tag{4}$$

All the quantities in Eq. (4) are functions of $E_{\max}$.

The total fission cross-section $\sigma(E)$ is obtained by integrating the differential cross-section,

$$\frac{d\sigma}{d\Omega}(\theta) = a + b\sin^2\theta + c\sin^2 2\theta \tag{5}$$

and the total cross-section is,

$$\sigma_0(E) = 4\pi\left(a + \frac{2b}{3} + \frac{8c}{15}\right)\,. \tag{6}$$

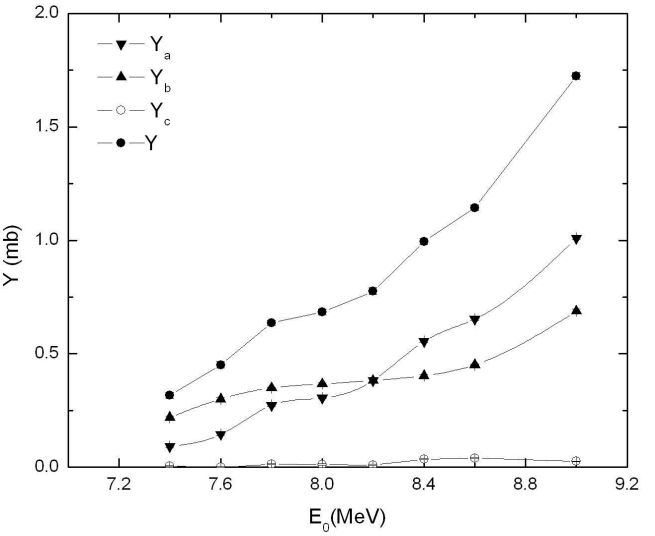

Fig. 6. Photofission yield of ^{238}U, Y, as a function of maximum bremsstrahlung energy.

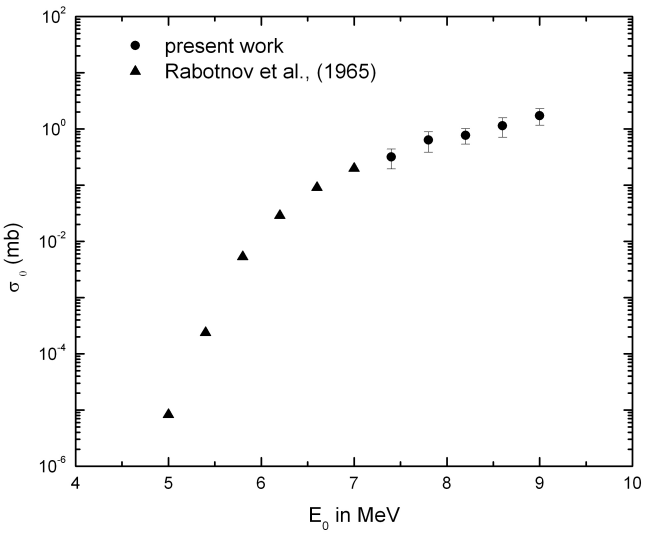

Fig. 7. Bremsstrahlung induced fission yield σ_0 of ^{238}U as a function of the maximum photon energy E_0.

The fission yield for a particular electron end point energy is related to fission cross-section ($\sigma(E)$) and bremsstrahlung gamma ray intensity ($N(E, E_{\max})$) by the relation,

$$Y(E_{\max}) = C \int_0^{E_{\max}} \sigma(E)/N(E, E_{\max})dE\,. \tag{7}$$

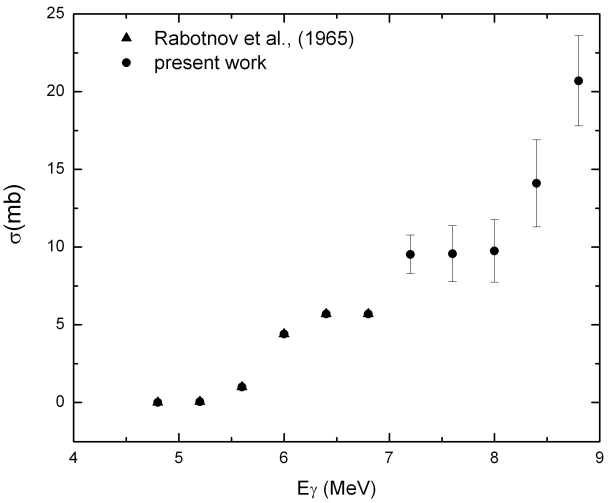

Fig. 8. Photofission cross-section of ^{238}U, σ, as a function of photon energy, E_0.

In the above equation, the "C" depends on the normalization of the spectrum and on the total number of fissile nuclei in the sample and on the total flux of incident photons. The resulting fission cross-section is obtained using photon difference method or iterative method or minimum directional discrepancy. In the present work, photon difference method has been employed to calculate the photofission cross-section. The photofission cross-section evaluated from the measured values is discussed below. The photofission excitation function was determined in the photon energy range 7.4–9.2 MeV. The fission yield for particular electron end point energy is related to fission cross-section ($\sigma(E)$) and bremsstrahlung gamma ray intensity ($N(E, E_{\max})$) [Eq. (7)].

The photofission yield has been obtained from the measurement of fission fragment angular distribution of ^{238}U in the energy range 7.4–9.2 MeV. Katz *et al.*[20] found the photofission threshold of ^{238}U to be 4.6 MeV. The photofission yield of bremsstrahlung end point energy is the contribution of photons from threshold to end point energy. To evaluate the resulting photofission cross-section, it is necessary to have the knowledge about the photon spectrum. In the present investigation, measurement data is available in the energy range 7.4–9.0 MeV; but below 7.4 MeV to threshold data is not available. Data from the studies carried out by Rabotnov *et al.*[3] was used for photofission cross-section measurements for the energy range 7.4 MeV up to threshold and were multiplied with bremsstrahlung spectrum $N(E, E_{\max})$ obtained by EGS-4 code,[12] to obtain the yield curve which is represented by solid triangle for energies below 7.4 MeV in Fig. 7 along with the yield curve of the present measurements. The yield curve of the present measurement is in good agreement with the Rabotnov *et al.*[3] photofission yield. The total yield curve is unfolded using photon difference method.[21] The resulting photofission

cross-section in the entire energy range 4.6–9.2 MeV is shown in Fig 8. The measured photofission cross-section is compared with the results reported in literature and are shown in Figs. 9–11.

The resulting photofission cross-section obtained in the present work indicates prominent resonance structure at 6.2 MeV and another resonance near 7.4 MeV.

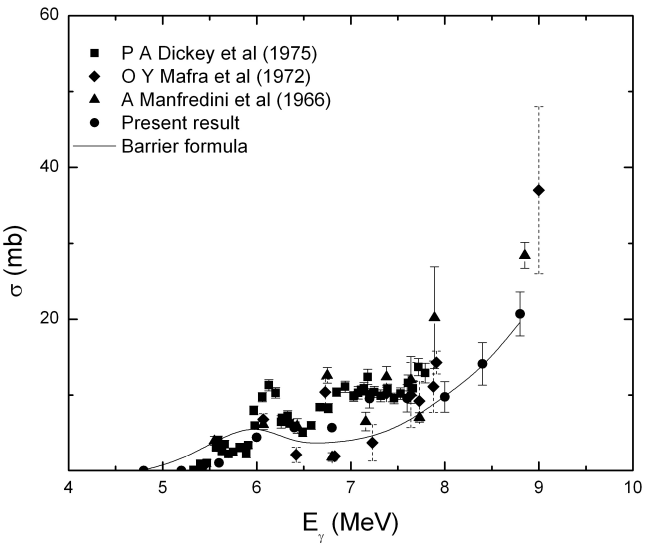

Fig. 9. Photofission cross-section of ^{238}U, σ, as a function of photon energy, E_γ.

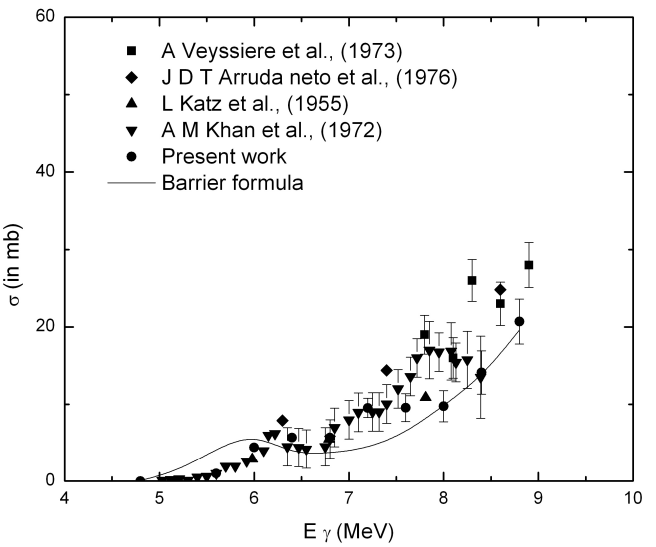

Fig. 10. Photofission cross-section of ^{238}U, σ, as a function of photon energy, E_γ.

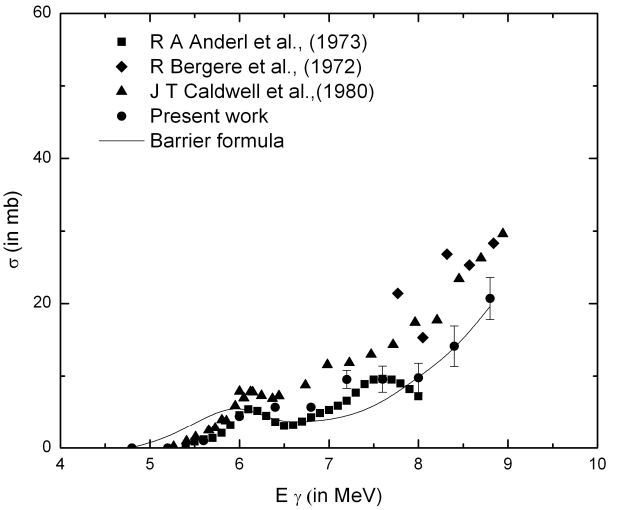

Fig. 11. Photofission cross-section of ^{238}U, σ, as a function of photon energy, E_γ.

Khan and Knowles[22] have used Compton-scattered γ-rays to measure the photofission cross-section of ^{238}U which we have compared with the present measurement in Fig. 10. Both cross-sections exhibit a large peak in the region of 6.2 MeV, but the two measurements do not agree above 7 MeV in excitation. Khan and Knowles[22] had considered that the photon beam striking the target could be assembled from discrete lines with an energy spread associated with each line and obtained cross-section from the yield by considering the presence of the discrete lines only. In their work, energy spread of each line was experimentally measured and was unfolded from the effective cross-section to get the actual cross-section. Smoothing was not applied during the analysis. To use the techniques employed by Khan and Knowles[22] the relative contribution to the scattered beam from each discrete line in the direct beam must be well known. In the present work, a representation of the beam could not be constructed in this manner since contaminant lines from the (n, γ) reaction on Fe and Al in the reactor contributes to the photon spectrum. The relative contribution of these non-localized sources to the overall intensity for each end-point energy is not known analytically. Hence, the photon spectrum was measured directly and was unfolded from the yield curves to obtain the cross-sections. Figures 9 and 10 show the data of Manfrenidi *et al.*,[23] Mafra *et al.*[24] who employed the same method as Khan and Knowles[22] and Fig. 11 shows data of Andrel *et al.*,[25] Caldwell *et al.*[26] who employed neutron-capture γ-rays as the photon source. The photon spectrum used in both of the above measurements consisted of discrete lines a few electron volts wide. Therefore, one must be careful in making a detailed comparison with these results since data are obtained at certain discrete energies only, and the photon energy may be on or off resonance with narrow states in the compound nucleus.

3.2. *Theoretical calculation of fission cross-sections*

In order to get a quantitative evaluation of the present experimental data, model calculations by using Empire-II code[6] for ^{238}U(γ, f) reactions was carried out. The parameters for the optical model were chosen by a global parameter set of Koning and Delaroche.[27] It should be noted that the level densities are important ingredients of statistical reaction models. The Empire code includes several level density models. Some of them are, (i) Gilbert–Cameron,[28] (ii) Fermi gas model with deformation-dependent collective effects, (iii) HF–BCS (Hartree–Fock–BCS approach).[29] The excitation energy dependence shell correction in the level density is given by Ignatyuk.[30] In the present work, calculations were done in the frame work of HFBCS model. The fission barrier height, width and transmission coefficient values were taken from the empire predictions of RIPL-1 and RIPL-2 (Reference Input Parameter Library). The RIPL-1 fission barrier parameters are compiled by Maslov nuclei beyond thorium systems while RIPL-2 fission barrier parameters are derived theoretically from the extended Thomas–Fermi plus Strutinsky integral (ETFSI) method.[31,32] The level densities at the saddles were calculated by using the Empire specific dynamical approach for normal states (BCS+ modified Fermi gas). No sub-barrier effects were included in the present calculation. However, discrete states above the fission barrier for nucleus are considered. The photoabsorption of both E1 (electric dipole) and E2 (electric quadrupole) are included in the present calculation. The calculation was carried out for ^{238}U(γ, f) reactions with the above set of parameters and the prediction of EMPIRE-II were compared with the present measurements and is shown in Fig. 12. The photofission cross-section has been calculated with newly developed analytical fission barrier formula[7] based on the

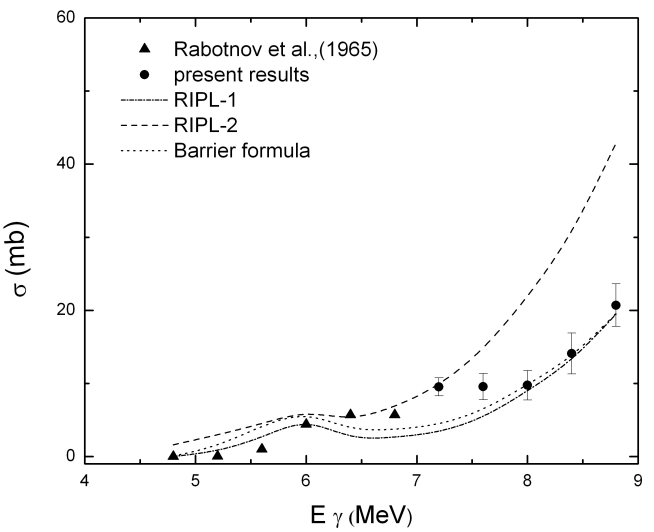

Fig. 12. Photofission cross-section of ^{238}U, σ, as a function of photon energy, E_γ.

Table 3. Values of the parameters used in the barrier formula.

$I = a/b$	a	b
B_{si}	0.03174	0.010290
B_{ci}	−0.01653	−0.06258
π	0.120 ± 0.023	-0.225 ± 0.029
υ	0.013 ± 1.2	0.044 ± 0.015
k	-10.3 ± 1.2	16.8 ± 1.9
δ_Z	-0.16 ± 0.06	-0.22 ± 0.08
δ_N	-0.32 ± 0.06	-0.22 ± 0.07
χ^2/degree of freedom	1.56	1.50

Table 4. Barrier heights and curvature for ^{238}U.

	V_a (MeV)	V_b (MeV)	$h\omega_a$ (MeV)	$h\omega_b$ (MeV)
RIPL-1	6.30	5.50	1.040	0.600
RIPL-2	5.70	4.90	1.040	0.600
Barrier formula	5.69	5.69	1.040	0.600

celebrated Hugenholtz–Van Hove theorem.[33] The pairing energy depends upon the single particle level density and varies along the potential energy curve. The analytical fission barrier formula for the barrier $V_I = a/b$ of the nucleus (A, Z, N) is given by,

$$V_i = a_s B_{si} A^{2/3} + a_c B_{ci} Z^{2/3} + \pi Z + \upsilon N + k + 1/2[1 + (-1)^Z]\delta_z + 1/2[1 + (-1)^N]\delta_N \,. \tag{8}$$

In the above equation, the first two terms (a_s and a_c) are the fitness terms — the surface and the coulomb. For the barrier formula parameters $a_s = 19[1 - (N - Z)/A)^2]$ MeV and $a_c = 0.72$ MeV was taken. The next three terms (π, υ and k) are the infinite matter terms satisfying the Hugenholtz–Van Hove theorem. The last two terms (δ_Z and δ_N) are the proton and neutron pairing terms. The surface and coulomb terms B_{si} and B_{ci} are taken from Brack *et al.*[34] and the remaining five parameters π, υ, k, δ_Z and δ_N are obtained by fitting the fission barrier data of Bjørnholm and Lynn[35] and are listed in Table 3.

The present measurement is also compared with the predictions of RIPL-1 and RIPL-2 fission barrier parameter of EMPIRE and analytical fission barrier formula and is shown in Fig. 12 and corresponding values of fission barrier used in the calculation are shown in Table 4.

4. Conclusion

Summarizing, we have measured the photofission cross-section of ^{238}U induced by bremsst'rahlung radiation of 7.4–9.0 MeV with the energy step of 0.4 MeV. The anisotropy decreases with increasing energy and quadrupole absorption is small,

but it systematically different from zero. The cross-section is obtained using photon difference method by unfolding present experimental measurements with the result obtained by Rabotnov *et al.* The theoretical photofission cross-section was estimated using Empire-II code using fission barrier parameter of RIPL-1 and RIPL-2 and a newly developed analytical formula for fission barrier. The present study shows that good agreement with the results obtained by a newly developed analytical formula for fission barrier and RIPL-1 from Empire-II. The present experimental results also compared with the results taken from literature, consistent with the experiment carried out using Bremsstrahlung gamma rays.

Acknowledgments

We thank Dr. S. Kailas and Dr. R. K. Choudhary for their keen interest. We are thankful to the Microtron technical staff for their help and cooperation during the course of this work. One of the authors, H. G. R. Prakash acknowledges the DAE-BRNS, Government of India, for the fellowship support to carry out this work.

References

1. S. J. Watson, D. J. S. Findlay and M. R. Sene, *Nucl. Phys. A* **548** (1992) 365.
2. G. N. Smirenkin and A. S. Soldatov, *Phys. Atom. Nucl.* **59** (1996) 203.
3. N. S. Rabotnov, G. N. Smirenkin, A. S. Soldatov, L. N. Usachev, S. P. Kapitza and Y. M. Tsipenyuk, *Phys. Lett. B* **26** (1968) 218.
4. R. Vandenbosch, *Phys. Lett. B* **45** (1973) 207.
5. J. W. Knowles, A. M. Khan and W. G. Cross, in Proc. 20th Annual Conference on Nuclear Spectroscopy and Structure of the Atomic Nucleus, January 28–February 5, *Izv. Akad. Nauk. SSSR Ser. Fiz.* **34** (1970) 1620.
6. M. Herman, P. Oblozinsky, R. Capote, A. Trakov, V. Zerkin, M. Sin and B. Carlson, EMPIRE-2.19, Nuclear Reaction Model, 22nd March, 2005.
7. S. K. Gupta and A. Saxena, in *Proc. of 8th Nuclear Data Workshop* (Pohang, South Korea, 2005).
8. www.nndc.bnl.gov.in for EXFOR files.
9. K. Siddappa, Ganesh, K. M. Balakrishna, S. S. Ramamurthi, H. C. Soni, P. Shrivastava, Y. Sheth and R. Hemnani, *Radiat. Phys. Chem.* **51** (1998) 441.
10. Y. N. Nagesh, Ganesh, K. C. Prashanth, D. Umakanth, A. P. Gnana Praksh, K. Siddappa and C. Srinivasan, *Indian J. Med. Phys.* **23**(3) (1999) 213.
11. Ganesh, K. C. Prashanth, Y. N. Nagesha, A. P. Gnana Prakash, D. Umakanth, M. Pattabi, K. Siddappa, S. Salkalachen and A. Roy, *Radiat. Phys. Chem.* **55** (1999) 461.
12. W. R. Nelson, H. Hirayanma and D. W. O. Rogers, The EGS code system (SLAC-Report-265, 1985).
13. K. M. Eshwarappa, Ganesh, K. Siddappa, Y. Kashyap, A. Sinha, P. S. Sarkar and B. K. Godwal, *Nucl. Instrum. Meth. A* **540** (2005) 412.
14. R. L. Fleischer, P. B. Price and R. M. Walker, *Nuclear Tracks in Solids: Principles and Applications* (University of California Press, Berkeley, 1975).
15. D. Umakath, R. V. Kolekar, Ganesh, P. Harisha, N. B. Nagesh, C. U. Prashanth, A. P. Gnana Prakash, V. B. Joshi and K. Siddappa, Estimation of photoneutrons from tantalum target using CR-39 detectors, in *Proc. Nat. Symp. of Radiation Physics* **14** (Gurunanak Dev University, 2001), pp. 482–485.

16. R. Vandenbosch and J. R. Huizenga, *Nuclear Fission* (Academic Press, New York, London, 1973), p. 116.
17. N. S. Rabotnov, G. N. Smirenkin, A. S. Soldatov, L. N. Usachov, S. P. Kapitza and Y. M. Tsipenyuk, *Nucl. Phys.* **77** (1966) 92.
18. A. P. Baerg, R. M. Bartholomew, F. Brown, L. Katz and S. B. Kowalski, *Can. J. Phys.* **37** (1959) 1418.
19. A. Bohr, On the theory of nuclear fission, in *Proc. 1st U.N. Int. Conf. Peaceful Uses of Atomic energy*, Vol. 1 (United Nations, New York, 1956), p. 151.
20. L. Katz, A. P. Baerg and F. Brown, *Second U.N. Int. Conf. Peaceful Uses of Atomic Energy*, Vol. 15 (United Nations, Geneva. 1958), p. 188.
21. L. Katz and A. G. W. Cameron, *Can. J. Phys.* **29** (1951) 518.
22. A. M. Khan and J. W. Knowles, *Nucl. Phys. A* **179** (1972) 333.
23. A. Manfredini, M. Muchnik, L. Fiore, C. Ramorino, H. G. De Carvlho, J. Lang and R. Muller, *Nucl. Phys.* **74** (1965) 377.
24. O. Y. Mafra, S. Kuniyoshi and J. Goldemberg, *Nucl. Phys. A* **186** (1972) 110–126.
25. R. A. Andrel, M. V. Yester and R. C. Morrison, *Nucl. Phys. A* **212** (1973) 221.
26. J. D. T. Arruda-Neto, S. B. Herdade, B. S. Bhandari and I. C. Nascimento, *Phys. Rev. C* **14** (1976) 1499.
27. A. J. Koning and J. P. Delaroche, *Nucl. Phys. A* **713** (2003) 231.
28. A. Gilbert, F. S. Chen and A. G. W. Cameron, *Can. J. Phys.* **43** (1965) 1248.
29. P. Demetriou and S. Goriely, *Nucl. Phys. A* **695** (2001) 95.
30. A. V. Ignatyuk, K. K. Istekov and G. N. Smirenkin, *Sov. J. Nucl. Phys.* **29** (1979) 450.
31. A. Mamdouh, J. M. Pearson, M. Rayet and F. Tondeur, *Nucl. Phys. A* **679** (2001) 337.
32. A. Mamdouh, J. M. Pearson, M. Rayet and F. Tondeur, *Nucl. Phys. A* **644** (1998) 389.
33. N. H. Hugenholtz and L. Van Hove, *Physica* **24** (1958) 363.
34. M. Brack, J. Damgaard, A. S. Jensen, H. C. Pauli, V. M. Strutinsky and C. Y. Wong, *Rev. Mod. Phys.* **44** (1972) 320.
35. S. Bjørnholm and J. E. Lynn, *Rev. Mod. Phys.* **52** (1980) 725.
36. E. J. Dowdy and T. L. Krysinski, *Nucl. Phys. A* **175** (1971) 501.